

Simple and Prospective Refractive Index Sensor involving Trapezoidal Index Profiles in the context of Splice Loss Analysis and Identification of appropriate profile

Jayee Sinha*, Ivy Dutta, Anirban Roy Chowdhury and Somenath Sarkar

Department of Electronic Science, University of Calcutta, 92 Acharya Prafulla Chandra Road, Kolkata 700009, India

Abstract. In this paper, we investigate, extensively, the effect of aspect ratio on the splice loss due to certain longitudinal misalignment at the joint between two single mode trapezoidal index fibers of identical aspect ratio. From this study, we report that as the value of aspect ratio decreases from 1.0 to 0.0, the splice loss increases, considerably, and, hence, triangular index fiber exhibits maximum loss. Further, the effect of refractive index of the index matching fluid filling the gap between two identical single mode triangular index fibers in reducing the splice loss is investigated and simple empirical relation for refractive index in terms of splice loss is prescribed to predict the refractive index of a medium from the direct knowledge of splice loss. Thus, we propose a method to study the prospective and possible use of the loss-sensitive triangular index profile as a refractive index sensor based on our empirical relation. We also show that even if there is a little digression from triangular index profile during fabrication, the system users can still confidently apply and use our empirical relation. The physical significance of our results is justified from basic diffraction ideas. Also, our refractometric formulation involving single mode fiber is simpler than the deeply involved relations of the recently proposed longitudinally displaced refractometer based on multimode fibers.

1 Introduction

Today importance of single mode fibers (SMF) as media in fiber optics communication and associated fiber optic devices [1-2] does not need any introduction. Together with dual mode fibers, they are important in fiber optic sensing systems [3-5]. In addition to the lowest loss window of glass at $\lambda = 1.55 \mu\text{m}$, these fibers can exhibit low dispersion by shifting of zero dispersion wavelength from $1.3 \mu\text{m}$ to $1.55 \mu\text{m}$, that can be achieved by tailoring the

* Corresponding author: jseic@caluniv.ac.in

refractive index profile using dispersion-shifted and dispersion-flattened mechanisms around this wavelength. The step index SMF offering structural rigidity for monolithic refractive index distribution has emerged as the most useful low loss transmission medium for long distance optical communication. Also, the triangular index fibers (TIF), are, extensively, used as dispersion-shifted fibers (DSF) [6-7], in directional couplers [8], in various sensing systems [9-10] etc. The W-type fibers are, generally, used for designing dispersion-flattened fibers. Among these DSF fibers, there is, also, trapezoidal index fiber (TrIF) receiving wide attention in the field of high-speed telecommunication as it enjoys the combined merits of step index fiber (SIF) providing rigidity and TIF showing dispersion-shifted criteria [11 – 13].

Now, a detailed modal analysis is necessary for the study of propagation of optical signal through conventional SMFs and this leads to the prediction of the most important propagation parameter, the modal spot size. Once the modal spot size is known, various other propagation characteristics like dispersion, splice loss, bending loss, micro-bending loss, fractional modal power through the core etc. can be determined, easily. In this context, in addition to the Marcuse empirical relations for spot sizes in terms of different normalized frequencies, V for SIF [14] and graded index fiber (GIF) [15], similar type relations have been proposed, lately, for circular core trapezoidal index SMF (CCTISMF) [13].

Recently, using these relations, effect of aspect ratio on Kerr nonlinear optical processes in subwavelength diameter single mode TrIF has been studied [16]. Further, based on these formulations, simple and complete empirical relations to predict the angle of beam divergence in terms of normalized frequency and aspect ratio of CCTISMF for far-field characterization have been presented [17]. Very recently, these relations have also been used to propose another simple and efficient method to predict the unknown aspect ratio of a given CCTISMF based on splice loss analysis between two perfectly aligned SIF and TrIF [18]. In another recent work [19], a simple method for characterization of CCTISMF is proposed using the above-mentioned empirical relations [13] utilizing the splice loss analysis technique based on the knowledge of angular misalignment between two identical pieces of CCTISMFs. The importance of both these works on transverse misalignment [18] and angular misalignment [19] are highlighted, recently, by further studies in an in-depth review in two review research papers [20] and [21], respectively.

In this paper, we carry out an investigation involving splice loss of two identical CCTISMFs in the presence of longitudinal misalignment. For our calculations, we keep the normalized frequency, V values, at 95% and 70% of LP_{11} mode cut-off V values of CCTISMF [12] for each value of aspect ratio, S . This is in order to standardize the comparison of our results in similarly expected single mode operation. We report that for a certain longitudinal misalignment D , the CCTISMF with aspect ratio $S = 0.0$ corresponding to triangular index profile (TIP), suffers maximum loss. Also, for small deviation from TIP i.e. in the near TIP region, the difference in splice loss from that of $S = 0.0$ is nominal. Further, we study the effect of the refractive index of the index matching medium in the gap between two longitudinally misaligned identical CCTISMFs having TIP on splice loss and is able to prescribe an empirical relation to predict the refractive index of a medium, based on splice loss analysis. Our empirical formulations establish that one can devise a refractive index sensor involving TIF. However, it will be, almost equally, sensitive for nearing values of aspect ratio of CCTISMF. Some interesting deeper physical insights based on basic diffraction ideas are also presented in order to justify our results. Also, our formulation involving SMF is novel, simpler and directly approximate analytical than such refractometer using longitudinally displaced multimode fibers in the recent past [22]. Present paper is formatted with theory and analysis in the next section following results and discussions and conclusion.

2 Theory and analysis

2.1 Basic Formulations

The scalar wave equation (SWE) for the fundamental mode governing light propagation in a GIF under the weakly guiding approximation is given as [23]

$$\frac{d^2\psi(R)}{dR^2} + \frac{1}{R} \frac{d\psi}{dR} + a^2 (k_0^2 n^2(R) - \beta^2) \psi(R) = 0 \quad (1)$$

where $\psi(R)$ is the modal field solution in the core ; $R = r/a$ is the normalized radial coordinate and r and a are the radial coordinate and the core radius, respectively; $k_0 = 2\pi/\lambda$, λ being the free space wavelength. Here, β is the propagation constant.

The refractive index, $n(R)$ in Eq. (1) for a weakly guiding GIF [23] is given by

$$\begin{aligned} n^2(R) &= n_1^2(1 - \delta f(R)) \quad \text{for } 0 < R \leq 1 \\ &= n_2^2 \quad \text{for } R > 1 \end{aligned} \quad (2)$$

where n_1 is the refractive index along the axis of the core; n_2 is the uniform cladding refractive index. Here $\delta = (n_1^2 - n_2^2)/n_1^2$ and the profile shape function, $f(R) = R^q$, where q is the profile exponent. Again, $q = 1, 2$ and ∞ correspond to triangular, parabolic and step index profiles, respectively.

Now, for trapezoidal index profile (TrIP), the Fig. 1 shows the refractive index distribution. Again, $f(R)$ appearing in Eq. (2) for CCTISMF is given by

$$\begin{aligned} f(R) &= 0, \quad \text{for } 0 < R \leq S \\ &= \frac{R - S}{1 - S}, \quad \text{for } S < R \leq 1 \end{aligned} \quad (3)$$

where the aspect ratio of the trapezoid is represented by S , defined as the ratio of the upper base width, w of the trapezoid to its lower base width, a which is also the core radius of the fiber and given by

$$S = \frac{w}{a} \quad (4)$$

Here, $S = 0$ and 1 give the triangular and step index profiles, respectively.

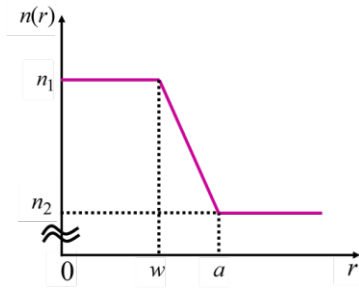


Fig. 1. Refractive index distribution for Trapezoidal Index Profile ($S = w/a$)

Using $n(R)$ defined in Eq. (2) in Eq. (1), we get the SWE as [23]

$$\frac{d^2\psi(R)}{dR^2} + \frac{1}{R} \frac{d\psi}{dR} + \left(U^2 - V^2 f(R) \right) \psi(R) = 0 \quad \text{for } 0 < R \leq 1 \quad (5)$$

where U and V are normalized propagation constant and normalized frequency, respectively.

Now, using the form of $f(R)$ for CCTISMF as given by Eq. (3) in Eq. (5), it yields two equations in two different regions of the core, given as

$$\frac{d^2\psi(R)}{dR^2} + \frac{1}{R} \frac{d\psi}{dR} + U^2 \psi(R) = 0 \quad \text{for } 0 < R \leq S \quad (6a)$$

$$\frac{d^2\psi(R)}{dR^2} + \frac{1}{R} \frac{d\psi}{dR} + \left\{ U^2 - V^2 \left(\frac{R-S}{1-S} \right) \right\} \psi(R) = 0 \quad \text{for } S < R \leq 1 \quad (6b)$$

Again, using Eq. (2) in Eq. (1) for the cladding region, where $f(R) = 1$, we get

$$\frac{d^2\psi(R)}{dR^2} + \frac{1}{R} \frac{d\psi}{dR} - W^2 \psi(R) = 0 \quad \text{for } R > 1 \quad (7)$$

where $W = \sqrt{V^2 - U^2}$ and is called the cladding decay parameter.

The modal field solution, $\psi(R)$ in the cladding for the above Eq. (7) is the analytical function given by the standard modified Bessel function as

$$\psi(R) = \psi(1) \frac{K_0(WR)}{K_0(W)} \quad \text{for } R > 1 \quad (8)$$

with $\psi(1)$ as the modal field solution at the core-cladding interface.

Now, it is well-known that the fundamental modal field for an infinitely extended parabolic index medium is, analytically, a Gaussian function. Hence, we can approximate the fundamental modal field for TrIF as [23]

$$\psi(R) = A e^{-R^2 / \omega^2} \quad (9)$$

where ω gives the normalized beam radius, up to which the field reduces to $1/e$ times the field amplitude at the core axis and is called the normalised spot size or the normalised mode field radius.

2.2 Analysis for estimation of normalised spot size of CCTISMF

Now, the fundamental modal spot size, ω of CCTISMF, as defined in the previous Sec. 2.1, can be obtained using a recent Marcuse-type formulation [13] that employs an optimization technique. In this formulation [13], at first, a set of optimum values of ω corresponding to V values are found for a particular value of S . The process is then repeated for different values of S ranging from 0 to 1. Then, applying an appropriate fitting procedure to these values, an empirical relation for ω in terms of V and S is obtained, given as

$$\omega = \sum_{i=0}^4 \frac{1}{V_i} \sum_{j=0}^4 A_{ij} S^j \quad (10)$$

where the A_{ij} coefficients are found using least square fitting procedure. The values of these A_{ij} coefficients are mentioned in Appendix A.

The Eq. (10) for evaluating ω for CCTISMF is valid for $1.5 < V < 5$ and is, also effectively, applicable for the two marginal values of the trapezoidal index fiber i.e., $S = 0$ and $S = 1$ for TIF and SIF, respectively.

2.3. Analysis for estimation of splice loss

Considering splicing between two identical CCTISMFs, for a longitudinal misalignment, D between the incoming and outgoing fibers, as shown in Fig. 2, a transmission power loss will be incurred.

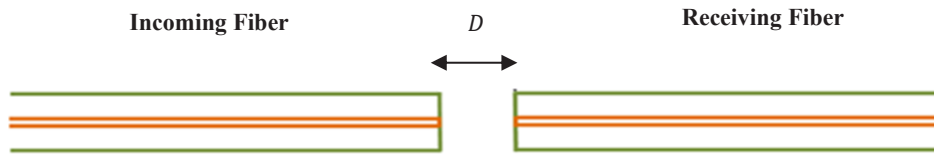


Fig. 2. Longitudinal misalignment, D at the splice between incoming and receiving fibers

For efficient coupling, the knowledge of this splice loss is essential, which can be obtained from the power transmission coefficient (PTC). This PTC in the presence of certain longitudinal misalignment, D between two identical SMFs is given by [23]

$$T_L = \left(1 + \frac{D^2 \lambda_0^2}{4\pi^2 n_L^2 \omega^4} \right) \quad (11)$$

where λ_0 is the free space wavelength, ω is the normalised spot size of the Gaussian field in each of the two identical CCTISMFs and n_L being the refractive index of the index matching medium in the gap between the two SMFs. In the present analysis, ω for the CCTISMF is obtained from Eq. (10) for different values of aspect ratio ranging from $S = 0$ to $S = 1$.

Now, the splice loss, α_L due to longitudinal misalignment, D can be obtained using Eq. (11) as [23]

$$\alpha_L = 10 \log(1 + \tilde{D}^2) \quad (12)$$

where the normalized longitudinal misalignment, \tilde{D} is given by

$$\tilde{D} = \frac{D\lambda_0}{2\pi n_L \omega^2} \quad (13)$$

The values of α_L obtained for different values of S using Eq. (12) are presented in the next section.

2.3.1. Diffraction concept for justification

Now, obtaining the values of α_L using Eqs. (12) and (13) due to certain D at the said gap for different values of V and S , we concentrate on comparison and interpretation of these values to select the appropriate aspect ratio, S , best suited for the possible use as a refractive index sensor.

In this connection, the basic diffraction ideas can be taken into account for physical justification of results. This is because the splice loss, α_L due to longitudinal misalignment is caused due to diffraction of the light wave as light propagates from one fiber end to the other one. This diffraction at the splice is sensitive to the optimized radial beam distance, d from the core axis because in the diffraction pattern, the half angular width of the central bright spot, following usual single slit diffraction formula is given by

$$\theta \sim \frac{\lambda}{d} = \frac{\lambda_0}{n_L d} \quad (\text{for small value of } \theta) \quad (14)$$

where, λ_0 is the wavelength of the propagating light wave in free space and λ is the wavelength of the same wave travelling through the index matching medium of refractive index, n_L .

For simple explanation, here, d is actually equal to our spot size, ω at core radius, which varies with the nature of RIP. In terms of Eq. (14), we will explain the results, physically, and establish the possible use of TIF as refractive index sensor that will be discussed in detail in the results and discussions section.

2.4. Empirical relation to devise a refractometer

It is clear from Eqs. (12) and (13) that the splice loss α_L depends both on the values of n_L and D . In the following section, we will show that for a certain D , the CCTISMF with extreme aspect ratio, $S = 0.0$ corresponding to TIP, suffers maximum loss out of all S . This loss maximisation is necessary for proper sensitiveness of fiber optic sensing system. This can be further utilised by considering different index matching media having different values of n_L in the gap between the two SMFs and studying how this affects the splice loss for a particular D value, when $S = 0.0$.

In this connection, it will be interesting to study the prospective possibility of designing a refractive index sensor by finding a formulation for the prediction of the refractive index of the index matching medium utilising the direct knowledge of maximum splice loss in case of TIF without requiring the knowledge of modal spot size, as no such method has been reported in literature till date to the best of our knowledge studying CCTISMFs. It may be relevant to mention that the recently proposed refractometer [22] showing emerging interest in literature

[22] utilizes two longitudinally displaced multimode fibers with presentation of deeply involved computations. Thus, the absence of such formulations for a TIF has motivated us to prescribe empirical relations involving n_L in terms of α_L and D on the basis of approximate analytical Gaussian formulation in SMF optics.

Using the value of normalized spot size ω for $S = 0.0$ i.e. TIF and a particular V value from the Marcuse type formulation given by Eq. (10), we obtain a set of values of α_L for different values of n_L for a particular value of D . Then, with these values, we apply a fitting procedure to our data and obtain an empirical relation of n_L with α_L . Then, we repeat this process with other values of D such that it yields the following fit,

$$n_L = a + \frac{b}{\alpha_L} + \frac{c}{\alpha_L^2} \quad (15)$$

where

$$\left. \begin{aligned} a &= a_1 D^{a_2} + a_3 \\ b &= b_1 D^{b_2} \\ c &= c_1 D^{c_2} \end{aligned} \right\} \quad (16)$$

Here, the values of the coefficients $a_1, a_2, a_3, b_1, b_2, c_1,$ and c_2 in Eq. (16) are determined by a proper fitting procedure and will be presented in Table 2 in Sec. 3.3 with proper mention.

3. Results and discussions

Now, for a particular value of n_L , we compute and present the values of splice loss, α_L due to longitudinal misalignment, D at the gap between two identical CCTISMFs for different values of S with a detailed comparison. Fortuitously, CCTISMF with $S = 0.0$ corresponding to TIF, earmarked as DSFs, exhibits maximum loss among all values of S ranging from 0.0 to 0.1. Utilizing this knowledge, we further present a detailed report on the study of the effect of the refractive index, n_L of the index matching fluid on the splice loss in between two identical CCTISMFs with certain longitudinal misalignment, D . Then, we elucidate the prospective and possible use of TIF as refractive index sensor following formulation of our empirical relation and verify these relations in an appropriate context. We, also, explore how much digression from the value of S of TIF can be allowed if there is any fault in the fabrication of the CCTISMF for which the empirical relation will be equally reliable.

3.1. Splice loss between two longitudinally displaced identical CCTISMFs

As stated above, we calculate and compare the values of α_L for different values of aspect ratio S of two given identical CCTISMFs. It is well known that the accurate knowledge of the LP₁₁ cut-off V values of the propagating fundamental modes through a fiber is essential for ensuring single moded operation. We follow the numerical method [12] proposed to evaluate the first higher order mode, LP₁₁ cut-off V values for different values of S for CCTISMF [12] and have considered these values in our present work. In order to ensure a standard comparison and single mode propagation of similar nature for each value of S of

the TrIP, calculations are carried out considering the values of normalized frequency V close to near cut-off region of CCTISMF i.e. at 95% and 70 % of the LP_{11} cut-off V values [12] for the respective values of aspect ratio ranging from $S = 0.0$ to $S = 1.0$. Here, we first consider air with $n_L = 1.0$ at the splice between the CCTISMFs and present a comparison of the values of splice loss from Eqs. (12) and (13) considering a particular value of $D = 1.0 \mu\text{m}$ in Table 1.

Table 1. Comparison of the values of longitudinal splice loss, α_L for different aspect ratios with $D = 1.0 \mu\text{m}$ and $n_L = 1.0$

S	V (5% less than cut-off)	α_L	V (30% less than cut – off)	α_L
0	4.16243	0.752765	3.06705	0.202175
0.1	3.94896	0.742104	2.90976	0.204540
0.2	3.72524	0.684417	2.74491	0.197064
0.3	3.496665	0.601478	2.57649	0.180158
0.4	3.27265	0.510702	2.41143	0.157176
0.5	3.061755	0.423041	2.25603	0.132226
0.6	2.86919	0.344514	2.11414	0.108427
0.7	2.696195	0.277704	1.98667	0.087472
0.8	2.54230	0.223309	1.87327	0.070266
0.9	2.405780	0.180756	1.77268	0.056931
1.0	2.28456	0.148898	1.68336	0.046502

In Table 1, the first column shows different values of S of CCTISMF, including the two extreme values i.e. $S = 1.0$ for step index profile (SIP) and $S = 0.0$ for TIP. In the second and fourth columns, we mention the V values at 95% and 70%, respectively, of the LP_{11} cut-off V values [12] for each value of S .

Next, for $D = 1.0 \mu\text{m}$, we present the values of splice loss, α_L in the third and fifth columns of Table 1, obtained from Eqs. (12) and (13) corresponding to the respective V values considering air in the gap. It is observed from the tabular comparison of the results that α_L decreases, gradually, with increase in S from 0.0 to 1.0 and it is maximum for $S = 0.0$ i.e. TIF. Further, it is also clear from our results that in the close vicinity of TIP i.e. for $S = 0.1$, the difference in splice loss with that for $S = 0.0$ is nominal. This finding will help system designers to develop fiber optic sensing system using TIP due to its loss

sensitive merit. Thus, for small deviation from TIP of about 10 %, the splice loss may be, tolerably, consistent and hence the sensing system will operate, equally effectively, in the close proximity of TIP i.e. in the near triangular region also if there is any anomaly in fabrication.

Further, in order to complement our findings, graphically, we present the variation of α_L with D considering air between the two fibers in Figs. 3 and 4. In both the figures, we present the plots for three different values of S as $S = 0.0$, 0.5 and 1.0 corresponding to their V values fixed at 95% and 70% of respective cut-off V values for each S .

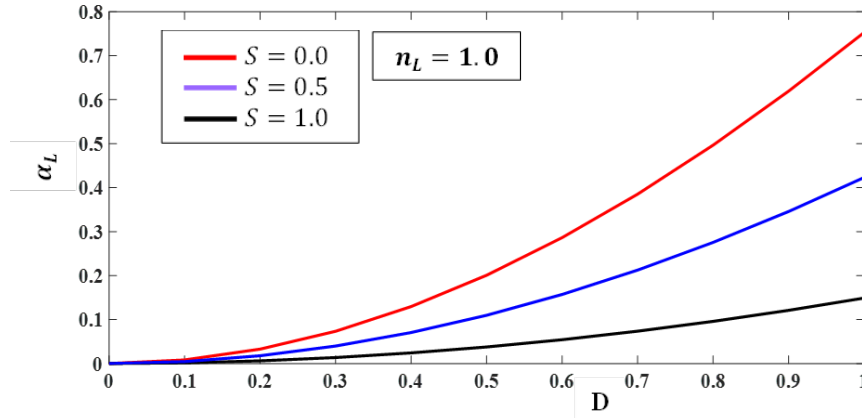


Fig. 3. Variation of longitudinal splice loss, α_L with longitudinal misalignment, D for V at 95% of their respective LP_{11} cut-off value for different aspect ratios

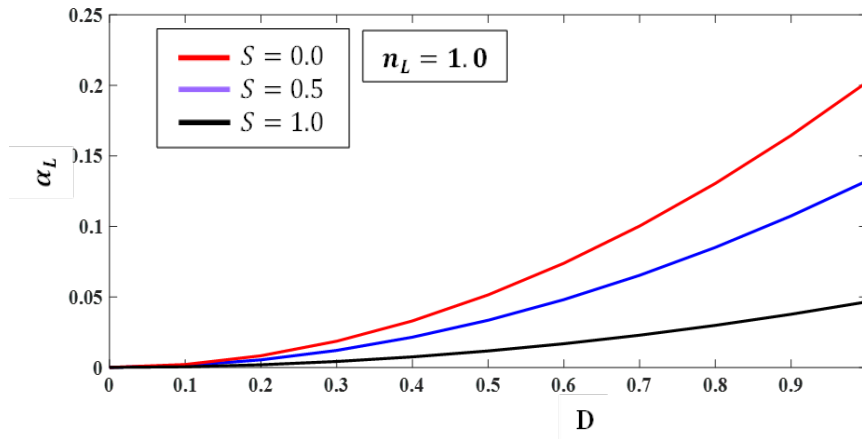


Fig.4. Variation of longitudinal splice loss, α_L with longitudinal misalignment, D for V at 70% of their respective LP_{11} cut-off value for different aspect ratios

It is seen from the above two Figs. 3 and 4 that the α_L values at the longitudinal gap between two identical CCTISMFs is maximum for the TIP ($S = 0.0$) and minimum for the SIP ($S = 1.0$) and it is quite obvious that the α_L increases with increase in D for every value of S . Further, loss, abruptly, falls when we operate at 70% of respective cut-off V values. So it is

judicious to operate the TIF as a refractometer operated at V value 95% of the LP_{11} cut-off V values. We discuss it in the next section.

3.1.1. Justification of results from basic diffraction consideration

In order to justify our results, physically, favoring TIP, we plot the fundamental modal field, $\psi(R)$ considering its Gaussian form as given by Eq. (9) with the normalized radial coordinate, R in Fig. 5. Here, first, we consider two extreme values of S as 0.0 and 1.0 corresponding to TIP and SIP, respectively, and an intermediate case for $S = 0.5$. We obtain the values of normalized spot size ω using Eq. (10) fixing the V value at 95% of the cut-off value for each value of S [12]. Then, using these values of ω in Eq. (9), we obtain the variation of the fundamental modal field by varying R . Here, we set the value of A which represents the axial field amplitude equal to 1 in Eq. (9). In Fig. 5, the black, the red and the green solid lines represent the fundamental modal field for SIP, TIP and TrIP with $S = 0.5$, respectively.

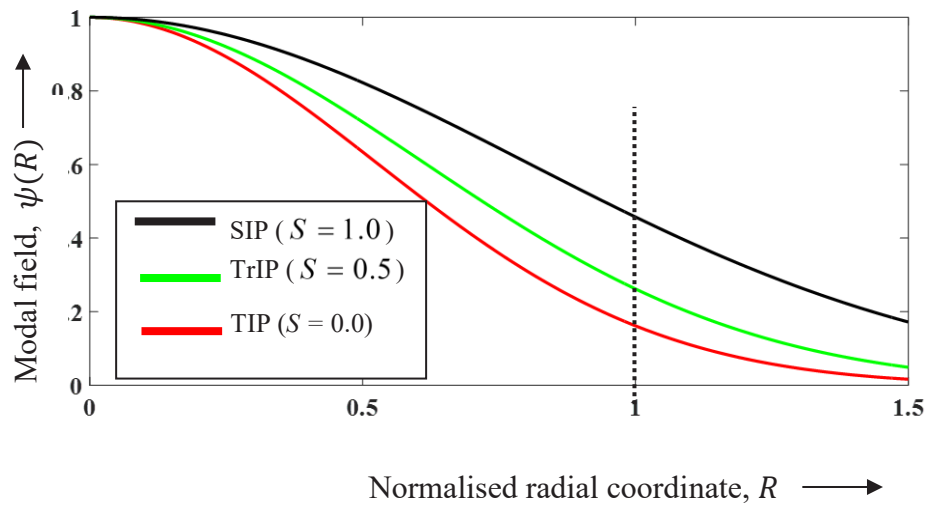


Fig. 5. Variation of fundamental modal field, $\psi(R)$ with radial distance from core axis

It is clear from Fig. 5 that the modal field decreases, rapidly, with radial coordinate in case of TIF compared to SIP. Thus the TIP confines the fundamental mode to a smaller beam radius, d around the core axis than a step-index profile does. Consequently, from Eq. (14), it is observed that, $d(\sim\omega)$ being effectively small in case of TIP compared to SIP, θ becomes high and hence the diffracted beam faces wider divergence in case of TIF. It explains the greater values of beam diffraction loss at the joint between two identical TIFs. Also, we can interpret for V values at 70% of its LP_{11} cut-off values, where for smaller value of V , ω is more and, hence, θ will be less in Eq. (14). Hence, as is expected, diffraction loss will be less leading to less splice loss, shown in Table 1.

Thus, since, TIF exhibits the maximum loss, we consider, in the next study, the effect of the index matching medium existing at the splice between the two SMFs on reduction in the splice loss.

3.2. Study of effect of refractive index of index matching medium on splice loss due to longitudinal misalignment

Now, in order to study and justify the effect of the refractive index of the index matching fluid on the splice loss for TIF as a special case of TrIF, we consider different values of refractive index, n_L of the index matching medium as $n_L = 1.0, 1.33, 1.46$ and 1.5 and present the variation of splice loss with D for these values of n_L in Figs. 6 and 7. Fig.6 is plotted considering the V value at 95% of LP_{11} , V cut-off frequency for TIF whereas, Fig.7 is plotted at 70% of LP_{11} , V cut-off value.

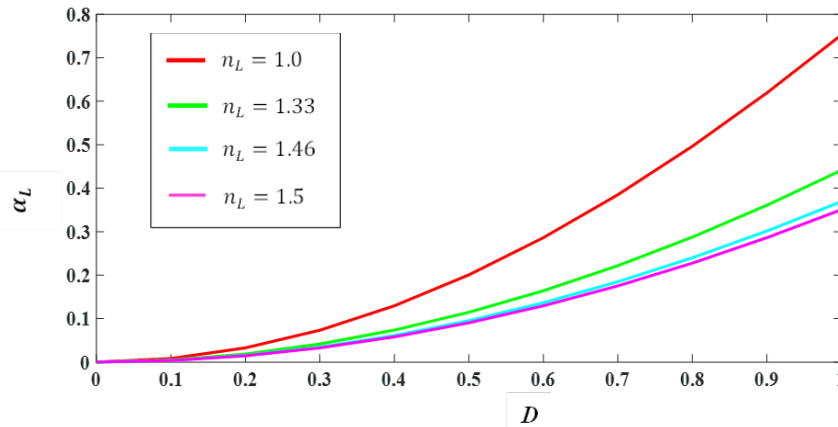


Fig. 6. Variation of α_L with D to show the effect of n_L for TIF with V at 95% of its LP_{11} cut-off frequency

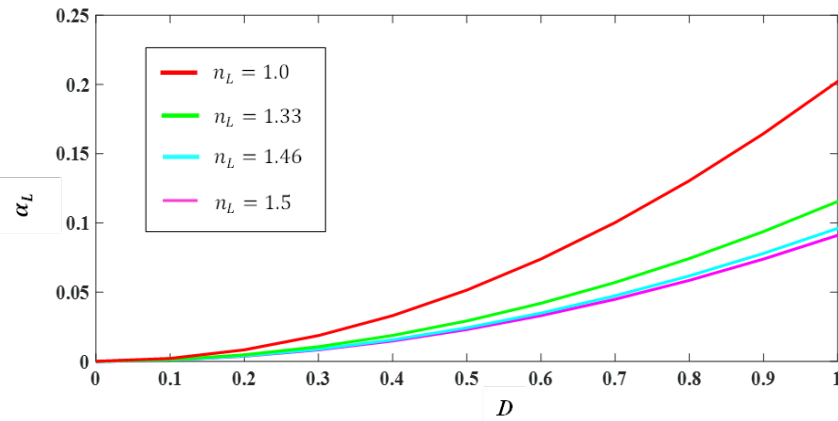


Fig. 7. Variation of α_L with D to show the effect of n_L for TIF with V at 70% of its LP_{11} cut-off frequency

Thus, from Figs. 6 and 7, it can be concluded that as the refractive index of the index matching medium, n_L increases, the splice loss is reduced, with minimum loss for $n_L = 1.5$. There is

an appreciable reduction in the splice loss for longitudinal misalignment when the value of n_L changes from 1.0 to 1.33. This can be appreciated from Eq. (14) where $n = n_L$ is the refractive index of the index matching medium. This n_L , being in the denominator, minimizes diffraction beam divergence, θ . However, the reduction in the splice loss for any value of D is very less as the value of n_L changes from 1.46 to 1.5.

Hence, once the splice loss between two identical longitudinally displaced TIFs is known experimentally, one can easily propose and develop a refractive index sensor in the context of TIF considering the effect of the refractive index of the index matching medium on the splice loss, as elucidated in our next study.

3.3. Estimation of the coefficients of our empirical formulations

Now, as stated before, we first compute the values of ω using the Marcuse type formulation given by Eq. (10) for TIP ($S = 0.0$) considering the corresponding V values at 95% of the LP₁₁ cut-off V value. We confine our attention to close to cut-off V values at 95% of LP₁₁ cut-off V values as it shows highest splice loss for TIF. Then, using these values of ω and considering a particular value of D , we calculate the values of α_L from Eqs. (12) and (13) by varying n_L from 1.0 to 1.5 in steps of 0.05. Next applying an appropriate fitting procedure to the reverse plot of n_L versus α_L for a particular D value, we obtain Eq. (15), and determine the coefficients a, b and c for this value of D . We repeat the above procedure for different values of D starting from $D = 0.1$ to $D = 1.5$ in steps of 0.1 corresponding to TIF yielding the values of the a, b and c coefficients for each value of D . Thus, each coefficient a, b and c of Eq. (15) depends on D and hence, we use a curve fitting procedure to obtain the proper fit, separately, for each of these coefficients in terms of D given by Eq. (16). For V value at 95% of LP₁₁ cut-off frequency value of TIF, the coefficients involved in Eq. (16) are given in the following Table 2.

Table 2. Values of coefficients involved in our empirical formulations for TIF at 5% less than V cut-off value

a_1	a_2	a_3	b_1	b_2	c_1	c_2
-0.05506	1.875	0.4615	0.5052	2.027	-0.04273	3.945

With these values of coefficients and empirical Eq. (15), we verify in the next section how much it is reliable.

3.4. Verification of our formulations and realization of refractive index sensor

Next, we consider the splicing between two identical CCTISMFs with certain longitudinal misalignment, D . As a test case, first, we consider a fixed value of n_L , say $n_L = 1.33$, to cross-check our formulations valid for TIF. To start with, we obtain the values of ω for TIP ($S = 0.0$) considering V values at 95% of the LP₁₁ mode cut-off value [12] for each S using

Eq. (10). Then, we repeat the same calculation for the near triangular profile, $S = 0.1$ and test its reliability. We present all these values of ω in the fourth column of Table 3. Next, considering the test value of n_L as 1.33, we calculate the values of α_L from Eqs. (12) and (13) with $D = 1.0 \mu\text{m}$ using the pre-determined values of ω and report these values in the fifth column of Table 3.

To verify our empirical formulations, we regenerate the value of n_L from Eqs. (15) and (16) using the above values of α_L and D and the coefficients mentioned in Table 2 and present the values in the sixth column of Table 3. Further, to be surer for the confirmation of the validity of our formulation, we choose two other values of n_L as 1.45 and 1.5. Following similar procedure, with $D = 1.0 \mu\text{m}$, we regenerate the values of n_L using Eqs. (15) and (16) and present them again in the sixth column of Table 3.

Table 3. Verification of our empirical formulations for TIP at 95% of LP₁₁ V cut- off value with its applicability for near TIP

Chosen n_L	S	V	ω	$D = 1.0 \mu\text{m}$		$D = 1.5 \mu\text{m}$	
				Values of α_L Eqs. (12) and (13)	Reproduced value of n_L from our empirical relations	Values of α_L [Eqs. (12) and (13)]	Reproduced value of n_L from our empirical relations
1.33	0.0	4.162425	0.740784	0.441445	1.331	0.936781	1.329
	0.1	3.948960	0.743665	0.434976	1.342	0.923783	1.339
1.45	0.0	4.162425	0.740784	0.374328	1.451	0.800980	1.448
	0.1	3.948960	0.743665	0.368801	1.462	0.789699	1.459
1.5	0.0	4.162425	0.740784	0.350753	1.499	0.752762	1.497
	0.1	3.948960	0.743665	0.345559	1.510	0.742104	1.508

For further verification of our formulations, we follow similar procedure with $D = 1.5 \mu\text{m}$ for V values at 95% of the LP₁₁ mode cut-off values for the same S values i.e. $S = 0.0$ and 0.1 and reproduce the previously chosen values of n_L and present them in the last column of Table 3.

Thus, from the first, sixth and last columns of the above Table 3, we see that our Eqs. (15) and (16), excellently, predict n_L for a perfect TIP. But, if we digress by 10% from $S = 0.0$, say for $S = 0.1$, these equations are still, excellently, reliable. This establishes the reliability of our empirical formulations for efficient prediction of the refractive index of the index matching medium, directly, from the knowledge of splice loss at the joint between two identical TIFs with a certain longitudinal misalignment. Also, even if there is any fault during fabrication that may cause digression from TIP, our formulation holds, fairly excellently, for the near TIPs. Thus, although the TIP is the most suitable profile due to its

high loss sensitivity, the same formulations can be applied for an allowable digression of approximately 10% to ensure fabrication tolerance, potentially leading to a trapezoidal profile rather than an ideal triangular profile.

Hence, if a splice loss experiment is performed with two identical pieces of TIFs, by knowing the splice loss arising due to a particular D between two identical TIFs for a fixed value of V with unknown index matching medium filling the gap between the two fibers, one can easily predict the value of n_L of the medium by direct application of our empirical formulations without requiring the knowledge of spot size. Thus, our empirical relation will serve the purpose of designing a refractive index sensor as it will be able to detect the value of n_L using the knowledge of splice loss. Further, our empirical formulations although prescribed for TIF, can be, effectively and safely, applied even if there is little deviation from TIP of about 10% from $S = 0.0$ for the V values at 95% of the LP_{11} cut-off value. Also, as mentioned earlier, the recently proposed refractometer based on two longitudinally displaced multimode fibers have presented deeply involved relations [22] whereas our prescription is straightforward and simple involving the modal theory of SMF, directly, without any approximation. Our proposal and formulations are novel and presented pedagogically so that any system user can design their experiment to follow them in user-friendly manner.

4. Conclusion

In this paper, we have reported a detailed study of the effect of refractive index, n_L of index matching medium in the gap between two longitudinally displaced identical CCTISMFs on splice loss due to longitudinal misalignment. We have shown that triangular index fiber with $S = 0.0$ exhibits maximum splice loss uniformly for all values of longitudinal misalignment, D and possess the best loss sensitive merit. Then, we have developed and presented empirical relations for n_L in terms of splice loss over a long range of D for V values of practical significance. We also show the excellent reproducibility of our result of n_L as compared with its initially chosen test value. We also observe that even if a small digression of the order of 10% from triangular nature with $S = 0.0$ occurs, high loss-sensitivity and our empirical relation is almost effectively valid. Thus, our empirical formula may find wide use as a ready reference by system users for easy computation and prediction of the refractive index of a medium based on splice loss analysis without requiring the knowledge of normalized spot size and thus will be useful in designing a refractive index sensor.

To confirm that a proposed refractive index sensing method is reliable and repeatable under real-world conditions, a combination of both controlled laboratory validation and practical, environment-driven testing might be necessary. This would help to show that the optical fiber sensor consistently produces accurate results despite being subjected to any anomaly, noise, variability and external disturbances. Also, testing related to accuracy and consistency of sensor outputs for different mediums with varying refractive index would lead to experimental validation when compared to known and exact values of refractive index of such mediums.

This research did not receive any specific grant from funding agencies in the public, commercial, or not-for-profit sectors.

The corresponding authors, on behalf of all authors, declare that there is no conflict of interest.

APPENDIX A

As reference for system users, we present below the values of the A_{ij} coefficients [13], stated in Eq. (10) to calculate the values of the normalised spot size of the given CCTISMF and the splice loss in Table A.1.

Table A.1. Values of A_{ij} coefficients [13] used for present calculation

j	A_{0j}	A_{1j}	A_{2j}	A_{3j}	A_{4j}
0	2.97989600312	-32.9392110273	162.3779206597	-330.21699698	264.51987438
1	-13.0506055408	161.301859211	-743.081536679	1487.3077079	-1140.377789
2	26.99553960765	-321.678223988	1442.922478411	-2843.7116046	2120.9331434
3	-24.66925975999	295.852162018	-1309.98446823	2556.1176787	-1873.080738
4	8.431920047329	-102.458402464	451.3106231284	-875.49410165	634.34159991

References

1. S. Sharma, A. Kumar, Analysis of Silica Based Single-Mode Fiber Doped with Germanium at Different Transmission Window, *Silicon* 14 (2022) 1023-1028.
2. Y. Chigusa, Y. Yamamoto, T. Yokokawa, T. Sasaki, T. Taru, M. Hirano, M. Kakui, M. Onishi, E. Sasaoka, Low-Loss Pure-Silica-Core Fibers and Their Possible Impact on Transmission Systems, *J. Lightw. Technol.* 23 (2005) 3541.
3. X. Wang, X. Sun, Y. Hu, L. Zeng, Q. Liu, J. Duan, Highly-sensitive fiber Bragg grating temperature sensors with metallic coatings, *Optik: Int. J. Light Electron. Opt.* 262 (2022) 169337.
4. H. Wan, J. Zhang, Q. Chen, Z. Wang, Z. Zhang, An active fiber sensor based on modal interference in few-mode fibers for dual-parameter detection, *Opt. Commun.* 481 (2021) 126498.
5. H. Zhang, Y. Li, B. Yuan, L. Meng, F. Cheng, Z. Yuan, H. Xue, Magnetic field sensor based on S-shaped and core-offset fusion splicing structure of single-mode fiber coated with magnetic fluid, *Optik: Int. J. Light Electron. Opt.* 245 (2021) 167630.
6. P. Nouchi, P. Sansonetti, J. Von Wirth, C. Le Sergent, New dispersion shifted fiber with effective area larger than 90 μm^2 , in *Proceedings of European Conference on Opt. Commun.* 1 (1996) 49-52.
7. Y. M. Liu, A. J. Antos, Dispersion-shifted large-effective-area fiber for amplified high-capacity long-distance systems, in *Proceedings of Opt. Fiber Commun. Conference* 3 (1997), 69-70.

8. P. Mohanraj, R. Sivakumar, Saturable higher nonlinearity effects on the modulational instabilities in three-core triangular configuration couplers, *J. Opt.* **23** (2021) 045502.
9. Z. Ding, C. Zhao, Fiber refractive index sensor based on Surface Plasmon Resonance in triangular pyramid structure, in 15th International Conference on Opt. Commun. and Networks (ICOON) **25** (2016) 1-3.
10. J. Yu, S. Xu, Y. Jiang, H. Chen, W. Feng, Multi-parameter sensor based on the fiber Bragg grating combined with triangular-lattice four-core fiber, *Optik: Int. J. Light Electron. Opt.* **208** (2020) 164094.
11. U. C. Paek, Dispersionless single-mode fibers with trapezoidal-index profiles in the wavelength region near 1.5 μm , *Appl. Opt.* **22** (1983) 2363-2369.
12. S. Behera, S.I. Hosain, P. Pattojoshi, Effect of on-axis dip in refractive-index profile on the cutoff frequency of modes of few mode fibers: a numerical approach, *Fiber and Integr. Opt.* **30** (2011) 112–124.
13. A. K. Mallick, S. N. Sarkar, Empirical relations to determine the normalized spot size of a single-mode trapezoidal index fiber and computation of its propagation characteristics, *Opt. Eng.* **53** (2014) 076103-1–076103-7.
14. D. Marcuse, Loss analysis of single-mode fiber splices, *Bell Syst. Tech. J.* **56** (1977) 703–718.
15. D. Marcuse, Gaussian approximation of the fundamental modes of graded-index fibers, *J. Opt. Soc. Am.* **68** (1978) 103-109.
16. G. P. Agrawal, *Nonlinear fiber optics*, Cambridge Massachusetts : Academic Press ; 2013.
17. J. Kang, S. Chen & W. Yang, Measuring far-field beam divergence angle of supercontinuum fiber sources, *Journal of Nonlinear Optical Physics & Materials*, **31**(04), (2022) 2350003.
18. A. R. Chowdhury, D. Kumbhakar, S. N. Sarkar, Characterisation of a single mode trapezoidal index fiber by splice loss technique using lateral offset, *Optik: Int. J. Light Electron. Opt.* **178** (2019) 403-410.
19. I. Dutta, D. Kumbhakar, S. N. Sarkar, Prediction of unknown aspect ratio of a single mode trapezoidal index fiber using splice loss technique considering angular misalignment, *Optik: Int. J. Light Electron. Opt.* **170** (2018) 132-139.
20. H. Zhou, H. Xu, J. A. Duan, Review of the technology of a single mode fiber coupling to a laser diode, *Opt. Fiber Technol.* **55** (2020) 102097.
21. H. R. Yang, L. Qiao, L. L. Xia, S. Xu , Y. C. Guo, Y. J. Zhang, Output error of converse piezoelectric fiber voltage sensor caused by optical fiber factors, *International J. Adv. Robotic Syst.* **16** (2019) 1-8.
22. D. Chetia, T. Basumatary, H. K. Singh, T. Bezboruah, Low-cost refractometer with longitudinally displaced optical fibers, *IEEE Sens. J.*, **16** (2016), 5950-5957.
23. A. Ghatak, K. Thyagrajan, *Introduction to Fiber Optics*, Cambridge University Press, Cambridge, UK, 2011.